J Mater Sci: Mater Med (2008) 19:343–357
DOI 10.1007/s10856-006-0024-y

Fibrinogen adsorption onto macroporous polymeric surfaces: correlation with biocompatibility aspects

A. K. Bajpai

Received: 20 May 2006 / Accepted: 19 October 2006 / Published online: 28 June 2007

Abstract The present work focus on the adsorption of fibrinogen (Fgn) on to the semi-interpenetrating polymer networks (IPNs) of polyethylene glycol (PEG) and poly(2-hydroxyethyl methacrylate-co-acrylonitrile) and attempts to correlate the adsorption behaviour of proteins to the blood compatible aspects of the polymeric surfaces. The semi-IPNs were prepared by copolymerizing 2-hydroxyethyl methacrylate and acrylonitrile in the presence of PEG and a crosslinker ethyleneglycol dimethacrylate (EGDMA). The prepared spongy gels were characterized by FTIR and Environmental Scanning Electron Microscopy (ESEM) for structural and morphological analysis. The prepared semi IPNs were studied for their water sorption capacity and the data were utilized to evaluate network parameters such as average molecular weight between crosslinks (M_c) and crosslink density (q). The adsorption of Fgn was carried out on to the prepared polymeric matrices and static and dynamic aspects of the adsorption process were investigated. The adsorption process was also studied as a function of pH and ionic strength of the protein solution and chemical architecture of the semi IPN. The antithrombogenic properties of the IPN's were also judged and correlated with water sorption and protein adsorption findings.

Introduction

Undesirable blood-polymer interactions are recognized problems in blood-contacting biomaterial devices such as catheters, vascular stents, artificial heart valves, and biosensors [1]. As soon as a material is placed within the body it is covered in blood due to the incision made in the surrounding tissue. The blood-material interaction starts a series of biological reactions (host responses) that in the best case lead to successful integration of the implant but in the worst case lead to a significant encapsulation [2].

The first event that takes place in nanoseconds at the implant–tissue interface is that water molecules and salt ions reach the material surface [3]. The distribution of these molecules and ions is highly surface dependent and is very important for proteins and other molecules that arrive later [4].

Shortly after the formation of hydration layer blood proteins and other macromolecules such as lipids, sugars etc. start to crowd the surface. Since blood contains several hundreds of different proteins, there will be a competition for the surface between the different species, resulting in unique protein mixtures at the interface.

In fact, protein adsorption onto biomaterial surfaces is believed to be the earliest event following implantation. This process is determined by the nature of the protein, the composition of the biological fluid, and the surface characteristics of the implanted device [5]. Conditioning with a protein layer can induce a series of consequential processes which may be beneficial or deterimental to the performance of the biomaterial. For instance, the binding of structural proteins such as albumin and globulines can improve the attachment of tissue cells, favouring the integration of a prosthesis into the host tissue [6]. Conversely, fibronectin and fibrinogen have been found to enhance the adhesion of bacterial species such as *Staphylococcus aureus*, a common cause of implant–related infection, onto polymeric biomaterials [7].

Of the numerous proteins available for investigation, fibrinogen has been studied most intensely due to its

A. K. Bajpai (✉)
Bose Memorial Research Laboratory, Department of Chemistry, Government Autonomous Science College, Jabalpur, MP 482 001, India
e-mails: akbmrl@yahoo.co.in; akbajpailab@yahoo.co.in

prominent role in coagulation and its ability to promote platelet adhesion [8]. Several studies have suggested that fibrinogen mediates platelet activation via its direct interaction with the platelet receptors GP IIb/IIIa, GP Ib, and possibly $\alpha_x\beta_3$ [9]. There are three distinct sites in the fibrinogen molecule that have been implicated to play a role in the binding of platelets. Two of them, the dodecapeptide (γ 400–411) and the RGPS sequence (A_α 572–575), which are located in the D-domain of the gamma chain are believed to be critical for platelet interaction with fibrinogen. Using monoclonal antibodies that bind to these functional regions, different groups have studied the accessibility of these sites when fibrinogen was adsorbed [10]. These observations suggest that certain conformations of adsorbed fibrinogen are more platelet adhesive than others which opens a possibility for creating a non-platelet adhesive substrate.

Materials for use in blood contacting devices often suffer from poor hemocompatibility compared to the natural endothelical vascular lining. A synthetic surface with improved biocompatibility would greatly improve the efficacy of blood contacting devices such as vascular grafts, heart valves, catheters and heart pumps. Although a variety of synthetic polymers like cuprophan, polysulphone, polyetherimide, polycarbonate block copolymers, etc. have been attempted in various blood–polymer interaction studies, the problem of thrombus formation on the polymer surface was always observed. This obviously hampers the clinical success of blood-contacting devices and make it necessary to use anticoagulants [11]. Since platelet adhesion/activation is mediated by adsorbed plasma proteins, it is essential to study the adsorption of proteins on to the polymer surfaces prior to their possible uses as biomaterials for different specific applications. The adsorption profile of plasma proteins depends strongly on the physicochemical properties of the polymers such as surface wettability, surface charge density, hydrophilic to hydrophobic ratio, etc. [12]. Thus, a complete study of protein adsorption is highly desirable not only for gaining insights into the protein–polymer interaction but also for predicting the possibility of using the polymer as a biomaterial for short and long term applications.

Thus, a material surface which non-specifically repels all proteins is desirable to minimize surface contact activation and control biofouling. Such surfaces can be prepared in many ways. For instance, polymer coatings have been successfully designed to modify a variety of polymeric substrates such as polycarbonate [13], polypropylene [14], low-density polyethylene [15], polystyrene latex [16], as well as glass [17] and ceramic surfaces [18–20]. Moreover, various researchers have also investigated the potential use of adsorbed diblock and triblock copolymers for reduction of protein adsorption [21, 22]. Reduction of protein adsorption onto polymeric substrates can also be achieved through chemical binding of preformed polymer chains [23], i.e., polymer grafting, or in situ polymerization onto the surface [24], i.e., graft polymerization.

An alternate method for improving blood compatibility of surfaces includes improvement of the biomaterials surface via preparation of interpenetrating polymer networks (IPNs). In recent years, an increasing number of publications have reported the preparation of thermoplastic apparent IPNs to modify surface properties of polymeric materials for blood-contacting devices [25]. Roman and his colleagues have synthesized several IPNs by use of a segmented polyurethane urea, Biospan (BS) and vinyl pyrrolidone-dimethacrylamide copolymer (VP-DMAm) [26]. They demonstrated that the VP content of this IPN was an important factor for controlling protein adsorption. Decreased fibrinogen and y-globulin adsorption, and increased adsorption of albumin for these IPNs, was consistently demonstrated with increased VP content.

A promising approach aimed at controlling bio-fouling is the use of polyethylene glycol (PEG) which is well known for its 'protein-resistant' property. PEG is a neutral, hydrophilic polymer that effectively forms hydrogen bonds with water [27]. This structured water layer is thought to contribute to the protein resistance of PEG. Other factors proposed to contribute to the PEG's protein resistance include a steric exclusion mechanism involving surface mobility and the dynamics of PEG chains [28]. PEG is also non-toxic and FDA approved for use in biotechnology and consumer applications. Because PEG lacks the mechanical integrity, it could be coupled with other polymer matrices.

In the present work, an attempt has been made to design a biocompatible semi-interpenetrating polymer network (semi-IPN) of PEG and poly(2-hydroxyethyl methacrylate-co-acrylonitrile) P(HEMA-co-AN) and investigate the adsorption dynamics of fibrinogen onto the IPNs surfaces. The use of HEMA polymer as one of the components of the IPN lies in its high water content, non-toxicity and favourable tissue compatibility which leads to a great number of biomedical applications [29, 30]. On the other hand, acrylonitrile polymers are well known for their mechanical strength, thermal stability and inertness to a wide range of solvents [31].

Experimental

Materials

Polyethylene glycol (PEG) (mol. wt. 6000) was obtained from S. Merck (India) and used as received. Acrylonitrile (AN) obtained from Loba Chemie, India was purified by washing the monomer successively with 10% NaOH, 10%

H_2SO_4 and distilled water, respectively and distilling it under vacuum. First and last 20% fractions were discarded.

2-Hydroxyethyl methacrylate (HEMA) was obtained from Sigma Aldrich Co. and the monomer was freed from the inhibitor following a method reported in the literature [32]. The crosslinker used in polymerization of HEMA was ethylene glycol dimethacrylate (EGDMA) obtained from Merck, Germany and used as received. Potassium persulphate and potassium metabisulphite were of Loba Chemie, India and used as received. Ethylene glycol was used as a cosolvent. Fibrinogen (Fgn) was obtained from Sigma Aldrich Co., USA and used without any pretreatment. All other chemicals used were of standard quality and double distilled water was used throughout the experiments.

Purity of HEMA

The purity of distilled HEMA was determined by high-pressure liquid chromatography (HPLC). A Backmen System (Gold 127) equipped with a ultraviolet detector, a 25 cm × 4.6 mm id separation columns ODS (C_{18}), 5 μm particle size were used. The uv detector was set at 217 nm. The mobile phase was methanol–water (60:40 v/v) and the flow-rate was kept at 1 mL/min. All samples were diluted with pure methanol to 1/1,600. About 10 μL samples were injected for each analysis. Samples of known concentrations of methacrylic acid (MAA) and EGDMA were injected into the HPLC and the resultant chromatographs used to construct a standard curve of known concentrations versus area under the curve. The chromatograph showed three distinct peaks. The first peak, 3.614 min was identified as MAA. The next peak 5.503 min was the major peak due to HEMA monomer. The final peak, 15.3 min, was due to the crosslinker, EGDMA. The amounts of impurities of MAA and EGDMA in the monomer samples were found to be less than 0.01 mol% MAA and 0.001 mol% EGDMA.

Methods

Synthesis of semi IPNs

IPN's were synthesized by a redox polymerization method as described elsewhere [32]. In a typical experiment, into a petri dish (diameter, 4″, Corning) were added PEG 0.5 g, AN 48.6 mM, HEMA 32.9 mM, ethylene glycol 71.6 mM as a cosolvent, EGDMA 0.53 mM and water. The whole reaction mixture was degassed by purging dry N_2 for 30 min. For initiating polymerization reaction, a redox couple comprising of degassed solutions of potassium persulphate 0.04 M and potassium metabisulphite (0.3 mM) were added to the reaction mixture and polymerization was allowed to proceed for 24 h. The white spongy gels were formed which were allowed to swell in bidistilled water for a week so that unreacted monomers and chemicals were leached out. The swollen gel was cut into small circular discs and allowed to dry at room temperature for a week. Upon drying the gels changed into transparent buttons, which were stored in an air tight containers. In this way, a series of IPN's of varying compositions were prepared.

Swelling experiments

The dry gel buttons were allowed to swell in phosphate buffer saline (PBS, pH 7.4) and taken out after 7 days. Upon swelling, the gels again become spongy white. The white swollen gels were gently pressed in between the filter papers to remove excess water and weighed. The swelling ratio was calculated by the following equation,

$$\text{Swelling Ratio} = \frac{W_s}{W_d} \tag{1}$$

where W_s and W_d are the swollen and dry weights of the IPNs, respectively.

Adsorption experiments

The adsorption of Fgn onto the IPNs was performed by the batch process as reported in our other communications [33]. For adsorption experiments protein (Fgn) solutions were made in 0.5 M PBS at physiological pH 7.4. A fresh solution of Fgn was always prepared for every adsorption experiment. Prior to adsorption experiments, the IPN buttons were equilibrated with PBS for 72 h. The adsorption was then carried out by gently shaking a Fgn solution of known concentration containing preweighed and fully swollen gels. By taking fully swollen gels, the possibility of absorption of protein solution within the gel becomes minimum. The shaking was performed so gently that no froth was produced otherwise it would have formed an air–water interface. After a definite time period, the gels were removed and the protein solution was assayed for the remaining concentration of Fgn by a UV–spectrophotometric procedure (Systronics, Model No. 2201, India). The adsorbed amount of Fgn (μg cm^{-2}) was calculated by the following mass-balance equation:

$$\text{Adsorbed Fgn} = \frac{(C_o - C_e)V}{A} \tag{2}$$

where C_o and C_e being the initial and equilibrium concentrations of Fgn solution (μg/mL), V is the volume of protein solution and A is the surface area of the swollen IPNs, i.e., the adsorbent.

For studying the kinetics of the adsorption process, the amount of adsorbed Fgn was determined at predetermined time intervals.

Blood compatibility tests

A biomaterial is a substance used in prostheses or in medical devices designed for contact with the living body for the intended method of application and for the intended period [34]. Synthetic polymer, the most diverse class of biomaterials, are widely used in both medical and pharmaceutical applications, and they contribute significantly to the quality and effectiveness of health care. These applications range from use in a variety of implants or other supporting materials (e.g., vascular grafts, artificial hearts, intraocular lenses, joints, mammary prostheses, and sutures to utilization in extracorporeal therapeutics and other supporting devices (e.g., hemodialysis, blood oxygenation, intravenous lines and blood bags), controlled release systems (e.g., transdermal drug delivery patches, microspheres, and microspheres for targeted drug delivery devices for different routes of administration), and clinical diagnostic assays mainly as carriers and supporting materials [35].

To be biocompatible, materials used in medical applications must meet certain criteria and regulatory requirements. The surfaces of biomaterials are believed to play an important role in determining biocompatibility. For materials that come in contact with blood, the formation of clot is the most undesirable but frequently occurring event that puts restriction on the clinical acceptance of material as a 'biomaterial'. Therefore, certain test procedures have to be employed to judge the hemo-friendly nature of the biomaterials.

Clot Formation Test: The antithrombogenic potential of the IPN surfaces was judged by the blood–clot formation test as described elsewhere [36]. In brief, the IPNs were equilibrated with saline water (0.9% w/v NaCl) for 72 h in a constant temperature bath. To these swollen IPNs were added 0.5 mL of acid citrate dextrose (ACD) blood followed by the addition of 0.03 mL of $CaCl_2$ solution (4M) to start the thrombus formation. The reaction was stopped by adding 4.0 mL of deionized water and the thrombus formed was separated by soaking in water for 10 min at room temperature and then fixed in 36% formaldehyde solution (2.0 mL) for another 10 min. The fixed clot was placed in water for 10 min and after drying its weight was recorded. The same procedure was repeated for the glass surface and sponges of varying compositions and respective weights of thrombus formed were recorded by a highly sensitive balance.

Hemolysis Assay: Hemolysis experiments were performed on the surfaces of the prepared sponges as described elsewhere [37]. In a typical experiment, a dry IPN film (4 cm^2) was equilibrated in normal saline water (0.9% NaCl solution) for 24 h at 37 °C and human ACD blood (0.25 mL) was added on the spongy film. After 20 min, 2.0 mL of saline was added on the sponge to stop hemolysis and the sample was incubated for 60 min at 37 °C. Positive and negative controls were obtained by adding 0.25 mL of human ACD blood and saline solution respectively to 2.0 mL of bidistilled water. Incubated sample was centrifuged for 45 min, the supernatant was taken and its absorbance was recorded on a spectrophotometer at 545 nm. The percent of hemolysis was calculated using the following relationship;

$$\%\text{Hemolysis} = \frac{A_{\text{testsample}} - A_{(-)\text{control}}}{A(+)\text{control} - A(-)\text{control}} \quad (3)$$

where A = absorbance. The absorbance of positive and negative centres was found to be 1.764 and 0.048, respectively.

Characterization

FTIR spectra

The IR spectra of dry IPN was recorded on a Perkin-Elmer spectrophotometer (FTIR, Paragon 1000).

Environmental scanning electron micrograph (ESEM)

The surfaces of dry and swollen IPNs were examined by ESEM technique (STEREO SCAN, 430, Leica ESEM USA).

Results and discussion

Characterization of IPNs

Structural parameters

One important structural parameter characterizing crosslinked polymer is M_c, the average molar mass between crosslinks directly related to the crosslink density. The magnitude of M_c significantly affects the physical and mechanical properties of crosslinked polymers and its determination has great practical value. Equilibrium swelling is widely used to determine M_c. Early research by Flory and Rehner [38] laid the foundation for analysis of equilibrium swelling. According to the theory of Flory and Rehner, for a network:

$$M_c = -V_1 d_p \frac{(v_s^{1/3} - v_{s/2})}{\ln(1 - v_s) + v_s + \chi v_s^2} \quad (4)$$

where V_1 is the molar volume of water (mL mol^{-1}), d_p is the polymer density (g mL^{-1}), v_s is the volume fraction of polymer in the swollen IPN, χ is the Flory–Huggins interaction parameter between solvent and polymer.

The swelling ratio (weight of swollen IPN/weight of dry IPN) may approximately be taken as equivalent to $1/v_s$. Here, the crosslink density q is defined as the mol fraction of crosslinked units, i.e.,

$$q = M_o/M_c \tag{5}$$

where M_o being the molar mass of the repeat unit.

Some authors define a crosslink density, v_e, as the number of elastically effective chains, totally included in a network, per unit volume, v_e is simply related to q, since,

$$v_e = d_p N_A/M_c \tag{6}$$

where N_A is Avogadro's number.

Since the IPN in the present study contains copolymeric structure, the molar mass of the polymer repeat unit, M_o, can be calculated as

$$M_o = \frac{n_H M_H + n_{AN}\ M_{AN}}{n_H + n_{AN}} \tag{7}$$

where n_H and n_{AN} are the mol numbers of HEMA and AN and M_H and M_{AN} are the molar masses of HEMA and AN (g mol^{-1}), respectively.

The density of the polymer d_p was determined to be 1.18 g cm^{-3}. Other parameters such as V_1 and χ were noted from the literature. Using Eqs. (5), (6) and (7) the value of M_c, q and v_e have been calculated for the IPNs of varying compositions. The values are summarised in Table 1.

Table 1 Structural parameters of the IPNs of varying compositions

PEG (g)	HEMA (mM)	AN (mM)	EGDMA (mM)	M_c	$q \times 10^3$	$V_e \times 10^{-20}$
0.5	32.9	48.6	1.06	2,818	29.8	2.6
1.0	32.9	48.6	1.06	2,210	38.0	3.3
1.5	32.9	48.6	1.06	1,824	46.0	4.0
2.0	32.9	48.6	1.06	1,432	58.6	5.1
0.5	16.4	48.6	1.06	3,218	12.3	2.2
0.5	24.6	48.6	1.06	3,048	25.8	2.4
0.5	32.9	48.6	1.06	2,818	29.8	2.6
0.5	41.1	48.6	1.06	2,422	37.6	3.0
0.5	32.9	16.2	1.06	2,088	49.8	3.5
0.5	32.9	32.4	1.06	2,466	36.9	2.9
0.5	32.9	48.6	1.06	2,818	29.8	2.6
0.5	32.9	64.8	1.06	3,284	23.6	2.2
0.5	32.9	48.6	0.53	3,082	27.2	2.3
0.5	32.9	48.6	1.06	2,818	29.8	2.6
0.5	32.9	48.6	1.59	2,440	34.4	3.0
0.5	32.9	48.6	2.12	2,188	38.3	3.3

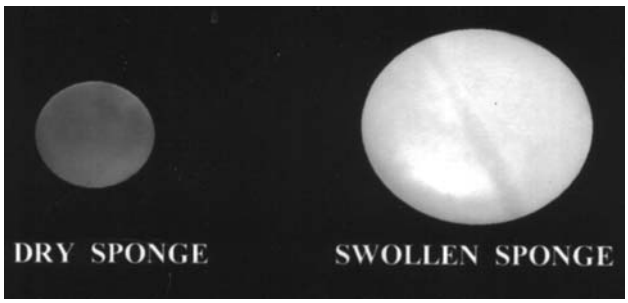

Fig. 1 A photograph showing the dry and swollen images of the semi-IPN

Appearance

During polymerization of HEMA, the phenomenon of phase separation occurs in the polymer system and as a result white and soft material is formed whereas in the dry state the material becomes hard and transparent. The dry and swollen IPNs are depicted in Fig. 1.

FTIR spectral analysis

The FTIR spectra of the semi-IPN of polyethylene glycol and poly(2-hydroxyethyl methacrylate-co-acrylonitrile) is shown in Fig. 2. The spectra clearly marks the presence of PEG in the IPN as evident from the observed absorption bands at 1,276 cm^{-1} (C–O stretching vibration in alcohol), 1,394 cm^{-1} (interaction between O–H bending and C–O stretching), and 1,112 cm^{-1} (asymmetric C–O–C stretching). The presence of HEMA is confirmed by the observed bands at 1,722 cm^{-1} (C=O stretching), 1,162 cm^{-1} (O–C–C stretching), 3,757 cm^{-1} (O–H stretching) and 1,456 cm^{-1} (O–H bending). Moreover, a broad peak observed at 3,399 cm^{-1} confirms the presence of intermolecular hydrogen bonded O–H stretch. The spectra also contains absorption bands in the range 2,273–2,000 cm^{-1} which are due to C≡N stretching of nitrile groups. The asymmetric stretch of methylene groups in the polymeric IPN is clearly seen at 2,936 cm^{-1}.

ESEM analysis

Surface topography and roughness are important factors in determining the response of cells to a foreign material [39]. Surface with grooves can induce "contact guidance", whereby the direction of cell movement is affected by the

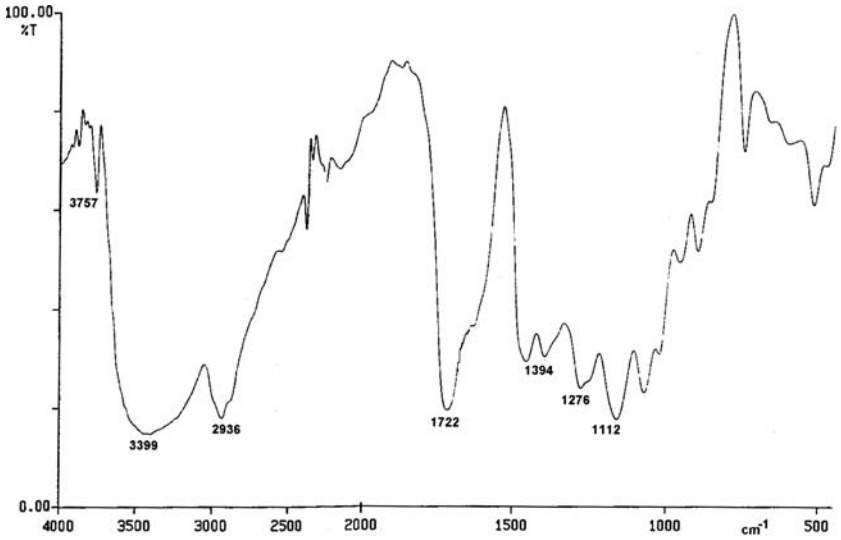

Fig. 2 FTIR spectra of the semi-IPN of PEG-P(HEMA-co-AN)

morphology of the substrate [40]. Likewise surface porosity has also been identified to affect the biocompatibility of polymeric biomaterials. Korbelar et al. [41] noticed an increase in biocompatibility of PHEMA hydrogels with increasing pore sizes of the surfaces.

In the present study, therefore, the porous nature of the IPN hydrogel has been confirmed by recording ESEM images of swollen gel as shown in Fig. 3. It is clear from the image that the swollen IPN surface presents well developed pores of size about 10 μm.

Swelling of the IPNs

Since high water content is sometimes a prerequisite of a biomaterial, the water sorption capacity of the IPNs have been determined as a function of the chemical composition of the IPNs. The swelling data are summarized in Table 2, which reveal that the degree of water sorption is greatly influenced by the chemical architecture of the IPN as discussed below:

When the amount of PEG is increased in the IPN in the range 0.5–2.0 g, the swelling ratio is found to decrease constantly. The observed decrease in water content may be attributed to the reason that although PEG is known for its water association property, its increasing concentration in the IPN results in a crowding of the PEG chains which causes a reduction of the pore sizes of the network. This obviously hinders the diffusion of water molecules into the network and thus lead to a fall in the swelling ratio of the IPN.

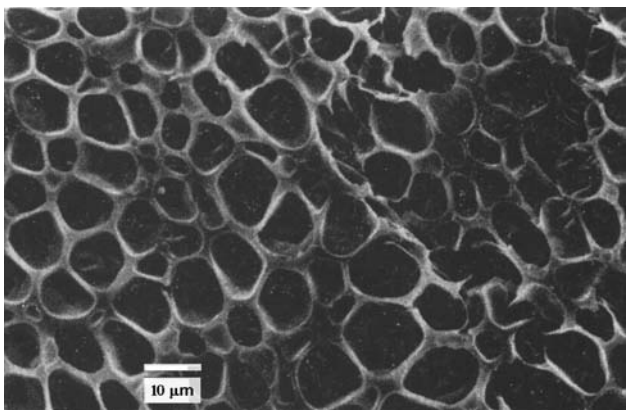

Fig. 3 Environment scanning electron micrograph (ESEM) image of the swollen IPN

Table 2 Data showing the water uptake by the semi-IPNs of varying compositions

PEG (g)	HEMA (mM)	AN (mM)	EGDMA (mM)	Swelling ratio
0.5	32.9	48.6	1.06	2.30
1.0	32.9	48.6	1.06	1.90
1.5	32.9	48.6	1.06	1.70
2.0	32.9	48.6	1.06	1.50
0.5	16.4	48.6	1.06	2.60
0.5	24.6	48.6	1.06	2.42
0.5	32.9	48.6	1.06	2.30
0.5	41.1	48.6	1.06	2.10
0.5	32.9	16.2	1.06	1.95
0.5	32.9	32.4	1.06	2.10
0.5	32.9	48.6	1.06	2.30
0.5	32.9	64.8	1.06	2.46
0.5	32.9	48.6	0.53	2.42
0.5	32.9	48.6	1.06	2.30
0.5	32.9	48.6	1.59	2.14
0.5	32.9	48.6	21.2	1.90

Although HEMA is a hydrophilic comonomer, however, with increasing concentration of it in the IPN in the range 16.4–41.1 mM, the swelling of the IPNs constantly decreases as shown in Table 2. The observed decrease in water sorption may be attributed to the reason that increasing length of polyHEMA segments in the network results in a dense network of copolymeric chains which consequently restricts the penetration of water molecules into the IPN thus decreasing the water sorption.

On the contrary an opposing trend has been noticed with increasing concentration of AN comonomer in the IPN as shown in Table 2. The results clearly reveal that with increasing AN in the range 16.2–64.8 mM the swelling ratio constantly increases. The enhanced water sorption may be attributed to the fact that because of the polar nature of the cyanide group in AN, an electrostatic repulsion operates between $-\overset{+\delta}{C} \equiv \overset{-\delta}{N}$ functional groups of the PAN segments thus widening the mesh size of the IPN. This clearly facilitates passage of water molecules into the network and, therefore, the degree of water sorption increases.

The crosslinker has a pronounced impact on the swelling behaviour of the IPNs as shown in the Table 2. When the concentration of EGDMA is raised in the feed mixture in the range 0.53–2.12 mM, the degree of water sorption decreases which is an usual observation. The decrease noticed in the swelling ratio of the IPN may be attributed to the reason that high amount of crosslinker produces a compact network with greater number of crosslinks. Thus, because of higher crosslink density, the pore sizes of IPN decrease which result in a lower degree of swelling. Another explanation for the observed fall in the swelling is that the introduction of crosslinker increases the glass transition temperature (T_g) of the polymer which obviously lowers the amount of water sorption. Similar type of results have also been published elsewhere [42].

Protein–surface interactions

In protein surface interactions, the governing forces are determined both by the physical state of the material and protein surface and the intimate solution environment. Factors including bound ions, surface charge, surface roughness, surface elemental composition and surface energetics, etc., all have to be considered in defining the role of the solid-solution interface [43].

Most surfaces acquire some charge when exposed to ionic solutions. In such cases the electrostatic interaction, which is long-ranged, will dominate protein adsorption kinetics. Because of the long ranged nature of the electrostatic interactions protein may be guided into a unique orientation when approaching the oppositely charged surface. Although a charged protein is expected to prefer adsorption on to an oppositely charged surface, the osmotic pressure of counter ions, charged group desolvation and burying of the charges into a low dielectric medium may, in fact, counteract protein adsorption. If considered alone, electrostatic interactions may not fully account to attachment of proteins to the charged interface. In the case of like charges between the surface and a protein an energy barrier to adsorption may develop. If the overall charge of protein is zero, i.e., at isoelectric point, the electrostatic interaction between protein and surface may still exist, because the charge distribution on the protein surface is not uniform.

Proteins are large amphipathetic compounds possessing multiple functional groups on their hydrophilic and hydrophobic domains. In aqueous solution the hydrophobic portion is shielded from water whereas the hydrophilic part is exposed to the adsorbing surface. In a similar way, the polymer matrix may also contain hydrophilic and hydrophobic segments (or groups), which could interact with the adsorbing protein molecules. Thus, the interaction forces between protein molecules and polymer particles can be classified as hydrophobic interactions, ionic (or electrostatic bonding), hydrogen bonding, and van der Waals interactions.

In the present study whereas the polyethylene glycol, polyacrylonitrile and hydroxyl and carboxyl groups of each repeat unit of PHEMA impart hydrophilicity to the IPN matrix, the crosslinker EGDMA and α-methyl groups and backbone of PHEMA provide hydrophobicity and mechanical strength to the IPN. Thus, a combined effect of hydrophilic and hydrophobic interactive forces between the IPN and Fgn molecules may lead to their adsorption as modelled in Fig. 4.

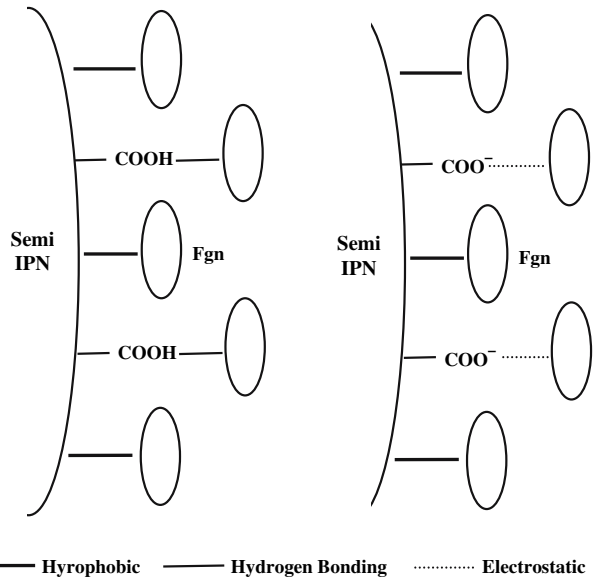

Fig. 4 A hypothetical model depicting the adsorption of Fgn onto the semi IPN surfaces

Modelling of protein adsorption isotherms

Many protein adsorption modelling approaches have been tried and several have been refined to be considerable successful [44]. Colloidal-scale models represent the protein as a particle and can accurately predict protein adsorption kinetics and isotherms. These colloidal scale models include explicit Brownian dynamics type models [45], random sequential adsorption models [46], scaled particle theory [47], slab models [48] and molecular theoretical approaches [49]. Most of these approaches treat the electrostatistics and van der Waals interactions between the protein and the surface, and thus can capture dependencies on surface charge, protein dipole moment, protein size or solution ionic strength.

Although the correlation between the adsorbed protein and bulk concentration of protein solution has been dealt with many adsorption isotherm equations [50], however, the Langmuir equation has been the first choice of researchers because of its computational simplicity and ease of applicability to various adsorption data. In the present study, the following two empirical equations have been used:

The Freundlich adsorption isotherm

$$C_s = kC_b^{1/m} \tag{8}$$

contains two parameters. The constant k is a measure of the capacity of the adsorption and exponent (1/m) is a measure of the intensity of adsorption.

Another equation used is the linearized Langmuir equation:

$$\frac{C_b}{C_s} = \frac{C_b}{C_L} + \frac{1}{C_L}.K \tag{9}$$

where C_b and C_s are bulk and surface protein concentrations, C_L is monotonically reached limiting surface concentration and K is a parameter which describes the strength of interaction between the protein and the surface.

Generally speaking, proteins adsorb on any surface with only a few exceptions. The fractional coverage is, therefore, strongly dependent on the bulk concentration of proteins.

The effect of initial concentration of fibrinogen solution on the adsorbed amount of fibrinogen has been investigated by varying its initial concentration in the range 55–850 μg/mL. The results clearly indicate that the adsorbed amount gradually increases with increasing concentration of protein solution and ultimately attains a limiting value, which is indicative of the formation of a monolayer on the IPN sponges. The observed increase may be attributed to the fact that with increasing bulk concentration of protein solution, greater number of protein molecules arrive at the sponge–water interface and get adsorbed over the sponge surfaces.

A more quantitative information about the protein–surface interaction may be obtained by constructing an adsorption isotherm which is normally obtained by plotting the adsorbed amount of fibrinogen against the residual concentration of the protein solution. The adsorption isotherm obtained in the present case is shown in Fig. 5 which is a typical Langmuirian type of curve which is characterized by an initial rising portion followed by a plateau portion. Similar type of isotherms have been frequently reported in the literature [51]. The adsorption isotherm constants have been summarized in Table 3.

Effect of pH and ionic strength

The pH of an adsorption medium has a significant influence on the amount of adsorbed protein. The effect is much more observable particularly in those systems which involve ionic type of adsorbate and adsorbent surfaces. However, in the present case since the IPN sponge is non-ionic in nature, the effect of pH on adsorption is solely determined by the fibrinogen molecule whose net charge varies with the pH of its solution. The effect of pH on the adsorption of fibrinogen has been investigated by varying pH of the protein solution in the range 2.1–11.0. The results are depicted in Fig. 6, which clearly imply that a maximum

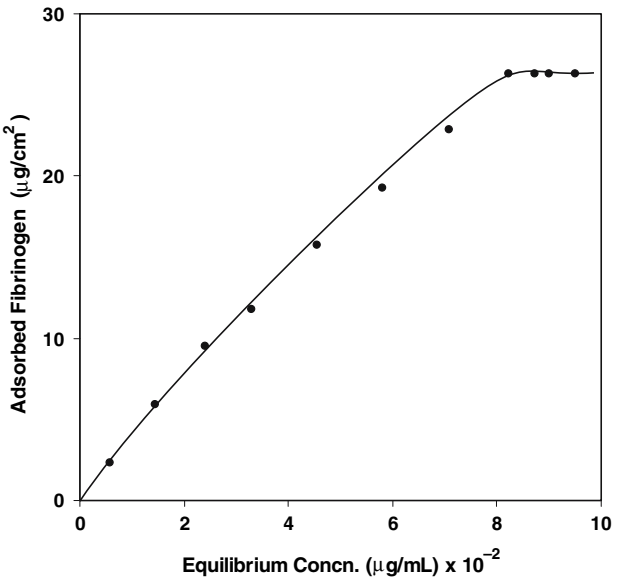

Fig. 5 Adsorption isotherm of the Fgn onto the IPN surfaces of definite composition [PEG] = 0.5 g, [HEMA] = 32.9 mM, [AN] = 48.6 mM, [EGDMA] = 1.06 mM, [Water] = 50% (v/v), [KPS] = 0.037 mM, [MBS] = 0.40 mM, pH = 7.4, Temp. = 37 ± 0.2 °C, Ionic strength = 0.001 M KNO_3

Table 3 Data showing various static and kinetic constants for adsorption of Fgn on to PEG-p(HEMA-co-AN) IPNs of definite composition

Parameters	Value
Freundlich constants	
(i) k	1.93
(ii) 1/m	0.69
Langmuir constants ($K \times 10^4$)	8.69
Rate constant for adsorption (k_1) $\times 10^6$	3.0
Rate constant for desorption (k_2) $\times 10^3$	1.0
Association constant (k_A) $\times 10^3$	3.0

[PEG] = 0.5 g, [HEMA] = 32.9 mM, [AN] = 48.6 mM, [EGDMA] = 1.06 mM, [$K_2S_2O_8$] = 0.037 mM, [Water] = 50% (v/v), pH = 7.4, Ionic strength = 0.001 M KNO_3, Temperature = 37 ± 0.2 °C

adsorption is noticed at pH 4.8, which is near to the isoelectric point of fibrinogen (5.1). The optimum adsorption of proteins at their isoelectric points is a common phenomenon in protein–surface interaction.

The observed optimum adsorption of fibrinogen at the isoelectric point may be because of the reason that at isoelectric point the lateral interactions between fibrinogen molecules are minimized and the protein acquires a compact conformation. Thus, greater number of fibrinogen molecules can adsorb on the given surface area of the IPNs.

An interesting feature revealed by Fig. 6 is that the adsorption isotherms constructed for various ionic strengths respond differently to pH of the adsorption medium. It is clearly shown in the figure that as the ionic strength increases the maxima present in the isotherm becomes more and more pronounced. The observed results may be attributed to the reason that at lower ionic strength, the density of fibrinogen molecules at the IPN-solution interface will be low and less number of protein molecules are operative at the active sites for adsorption. Thus, the lateral interactions among the molecules are not indifferent and significant at below and above the isoelectric point of the protein. As a consequence of this the adsorbed fibrinogen also does not vary appreciably, thus giving an isotherm of less pronounced maxima. On the other hand at higher ionic strength, greater number of fibrinogen molecules cause a greater degree of lateral interactions and, therefore, result in a pronounced maxima.

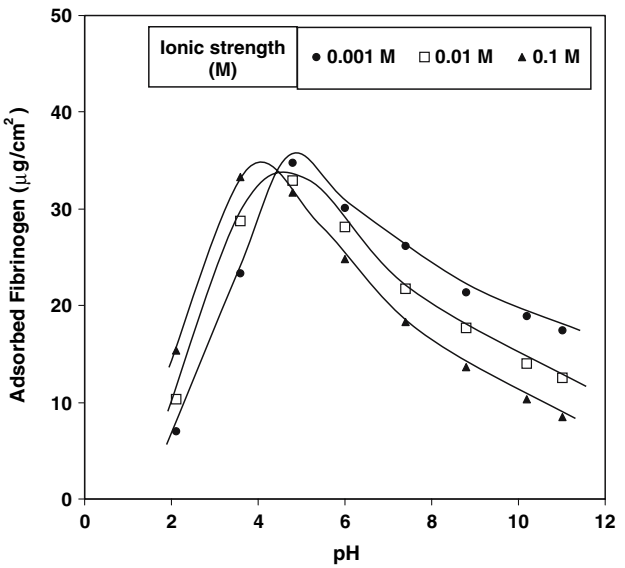

Fig. 6 Adsorption isotherm of the Fgn onto the IPN surfaces at different pH and ionic strengths the protein solution at fixed composition [PEG] = 0.5 g, [HEMA] = 32.9 mM, [AN] = 48.6 mM, [EGDMA] = 1.06 mM, [Water] = 50% (v/v), [KPS] = 0.037 mM, [MBS] = 0.40 mM, Temp. = 37 ± 0.2 °C

Another important observation is that the shape of the adsorption isotherm is appreciably affected by the ionic strength of the medium as shown in Fig. 6. It is implied by the results shown that in the acidic range the amount of adsorbed fibrinogen increases with increasing ionic strength of the medium. The observed increase may be due to the reason that with increasing ionic strength, the electrostatic repulsions decrease in the interior of protein molecules, which leads protein molecules to form more compact structures. Moreover, lateral repulsions between the adsorbed protein molecules also decrease with increasing ionic strength and, thus, greater number of molecules can adsorb on to the given surface area.

It is also revealed by the figure that the maxima at which the adsorption of fibrinogen becomes optimum is slightly shifted towards acidic pH range with increasing ionic strength. This shifting of the maxima has been observed earlier also [52].

Dynamics of Fibrinogen adsorption

Accurate knowledge of the adsorption kinetics under a given set of conditions is a prerequisite in elucidating the mechanisms of many fundamental biological processes. The adsorption of proteins from its aqueous solution onto a solid surface is normally considered to occur in three steps [53]: (i) diffusion of protein molecules from bulk to the interface, (ii) attachment of protein molecules to active sites on the surface, and (iii) reconformation of the structure of the protein molecule after adsorption. Of these steps, the step (iii) plays a significant role not only in controlling the adsorption kinetics of proteins, but also in modification of the surface properties of the substrate.

The dynamics of the adsorption process was followed by determining the amounts of adsorbed fibrinogen at various time intervals, as shown in Fig. 7. It is clear from the figure that the rate of adsorption is almost constant up to 10 min

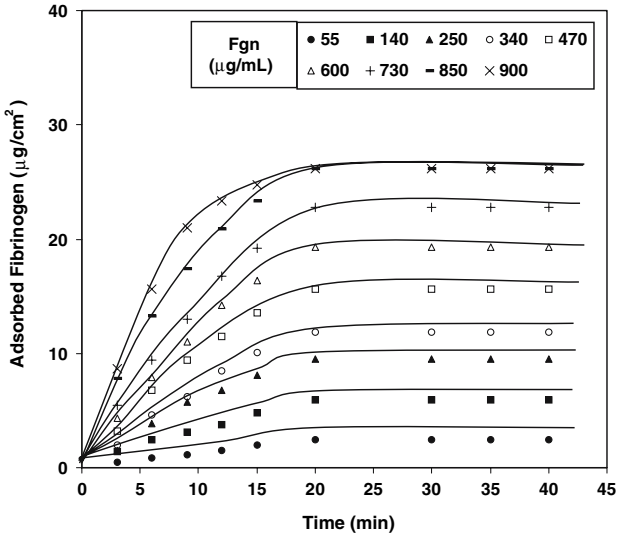

Fig. 7 Plots showing the progress of the adsorption process of varying Fgn solutions onto the IPN surfaces of definite composition [PEG] = 0.5 g, [HEMA] = 32.9 mM, [AN] = 48.6 mM, [EGDMA] = 1.06 mM, [Water] = 50% (v/v), [KPS] = 0.037 mM, [MBS] = 0.40 mM, pH = 7.4, Temp. = 37 ± 0.2 °C, Ionic strength = 0.001 M KNO_3

and then it gradually slows down attaining a limiting value after 20 min. The kinetic profile of the adsorption process may be explained by the fact that the adsorption of functionalized large chains (such as proteins) is a two regime process [54]. At the initial stages, the IPN surface is bare and the kinetics of adsorption is governed by the diffusion of the chains from the bulk solution to the surface. All the fibrinogen molecules arriving at the interface are considered to be immediately adsorbed. The mass transport can be interpreted as a Fickian diffusion. The diffusion coefficient can be determined by the following equation

$$q = \frac{2}{\pi} C_o \sqrt{Dt} \tag{10}$$

From the slope of the curve drawn between q (adsorbed fibrinogen) and √t, for the fibrinogen solution of varying concentrations, the diffusion constants can be calculated as summarized in Table 4. It is revealed by the data that with an increasing concentration of fibrinogen solution, the diffusion constants constantly decrease. The observed decrease may be attributed to the fact that as the bulk concentration of protein solution increases the fibrinogen molecules approaching at the substrate–solution interface have to go across a thicker protein layer near the interface and, therefore, diffuse slowly. Similar type of lower diffusion constant at higher protein concentration have also been reported [54]. This is expected from the Ficks law of diffusion since the concentration gradient at the sponge–solution surface increases with increase in the initial concentration of fibrinogen solution.

Table 4 Variation of diffusion constant (D) and penetration constant ($1/\tau$) with bulk concentration of protein solution

Fibrinogen concentration (μg/mL)	Diffusion constant $D \times 10^7$ cm^2 s^{-1}	Penetration constant $(1/\tau) \times 10^3$ s^{-1}
55	2.04	1.11
140	1.96	1.38
250	1.57	1.80
340	1.33	2.08
470	1.17	2.31
600	1.09	2.54
730	1.04	2.67
850	1.00	2.70

In the later stage of adsorption process a barrier of adsorbed molecules exists, and the molecules arriving from solution have to diffuse across this barrier. This penetration is slow, and a theoretical treatment given by Ligorue and Leibler predicts an exponential time dependence for the later stages [55]

$$q(t) = q_{eq}[1 - \exp(-t/\tau)] \tag{11}$$

where q_{eq} is the adsorbed amount at equilibrium and $1/\tau$ is the penetration rate constant (τ is also known as relaxation time). The above equation suggests that the second process has an exponential nature, and the penetration rate may be obtained from the slope of the plot of $[\ln(q_e - q)]$ as a function of time. From the slopes of the straight lines (not shown) the penetration rate constants for varying bulk concentration of fibrinogen solutions have been calculated and summarized in Table 4.

The results clearly reveal that the penetration constant ($1/\tau$) increases with increasing bulk and surface concentration of fibrinogen. The observed increase is quite obvious as at higher bulk and surface concentration, the protein molecules diffuse more slowly and thus require greater time for penetration to get adsorbed onto the sponge surface.

Kinetic model for adsorption

The kinetic model described by Tanaka and coworkers [56] may be successfully employed to investigate the dynamic nature of the adsorption process. In brief, the protein (fibrinogen) adsorption on polymer surface (IPN sponge) may be described by the following Eq. (12)

$$\begin{aligned}[\text{Polymer}] + [\text{Protein}] &\underset{k_2}{\overset{k_1}{\rightleftharpoons}} [\text{Polymer} - \text{Protein}]^* \\ &\underset{k_4}{\overset{k_3}{\rightleftharpoons}} [\text{Polymer} - \text{Protein}]\end{aligned} \tag{12}$$

In the above equation [Polymer – Protein]* represents the meta-stable complex composed of the polymer surface and the protein. In the early stage of protein adsorption, it is assumed that the reaction on the polymer surface can be simply described by the following Eq. (13), which reveals that the extent of adsorption depends on the amount of the complex.

$$[\text{Polymer}] + [\text{Protein}] \underset{k_2}{\overset{k_1}{\rightleftharpoons}} [\text{Polymer} - \text{Protein}] \tag{13}$$

On the basis of the above equation, the production rate of meta-stable complex can be given by the following equation.

$$\frac{d}{dt}[\text{Polymer} - \text{Protein}]^* = k_1[\text{Polymer}][\text{Protein}] - k_2[\text{Polymer} - \text{Protein}]^* \tag{14}$$

The amount of the complex formed at time t is given by Eq. (15)

$$[\text{Polymer} - \text{Protein}]_t^* = [\text{Polymer} - \text{Protein}]_\infty^* (1 - e)^{(-1/\tau)t} \tag{15}$$

where $[\text{Polymer} - \text{Protein}]_\infty^*$ is the concentration of the complex at theoretical time ∞, τ is the relaxation time of the adsorption, and the reciprocal of τ is defined by the following Eq. (16).

$$\tau^{-1} = k_1[\text{Protein}]_o + k_2 \tag{16}$$

where $[\text{Protein}]_o$ is the initial concentration of the fibrinogen. The complete derivation of the above equation may be seen in the Ref. [56]. The Eq. (16) clearly indicates that from the slope and intercept of the plots drawn between τ^{-1} and $[\text{Protein}]_o$, the values of k_1, k_2 and k_1/k_2 ($=k_A$) may be calculated. In the present study, the kinetic parameters calculated for the fibrinogen adsorption have been summarized in Table 3.

Effect of concentration on adsorption kinetics

The adsorption of fibrinogen is well known to exhibit different adsorption behaviour at low and high protein flux conditions [57], thus, indicating a history dependence on the ultimate surface coverage [58]. Initially, it was suggested that the fibrinogen can exist in two distinct conformations on surfaces, resulting in two experimentally observable populations; a larger irreversibly adsorbed layer on a smaller reversibly adsorbed layer [59]. However, recent studies have revealed that fibrinogen can exist in many possible orientations and/or conformations depending on the adsorption history and the surface chemistry of the substrate [57]. It was also shown that fibrinogen adsorbs non-specifically to both hydrophobic and hydrophilic surfaces, resulting in a random mixture of end-on and side-on oriented molecules initially. Following attachment to the surface fibrinogen begins to increase its foot print (i.e., the number of segment-surface contacts) in a manner that is consistent with denaturation (unfolding) on hydrophobic surfaces and reorientation (rolling over) on hydrophilic surfaces. Thus, reversibly and irreversible bound populations may consist of many different protein footprint sizes, not only as two distinct conformations.

Thus, realizing the impact of protein flux on the adsorption dynamics of fibrinogen onto the PHEMA sponge surfaces, the influence of bulk concentration of protein solution has been investigated on the dynamic nature of the adsorption process by monitoring the progress of the adsorption process at different bulk concentration varying in the range 950–1,200 μg/mL. The results shown in Fig. 8 are quite unusual and the adsorption profiles appear unlike any of the other protein. The results clearly reveal that whereas at low solution concentrations the adsorption reach at a plateau value (Fig. 7), at higher concentration range, i.e., from 950 μg/mL to 1200 μg/mL the adsorbed amount of fibrinogen attains an optimum value and, thereafter, decreases with increasing time. Similar type of results have also been published elsewhere60. The results can be interpreted as below.

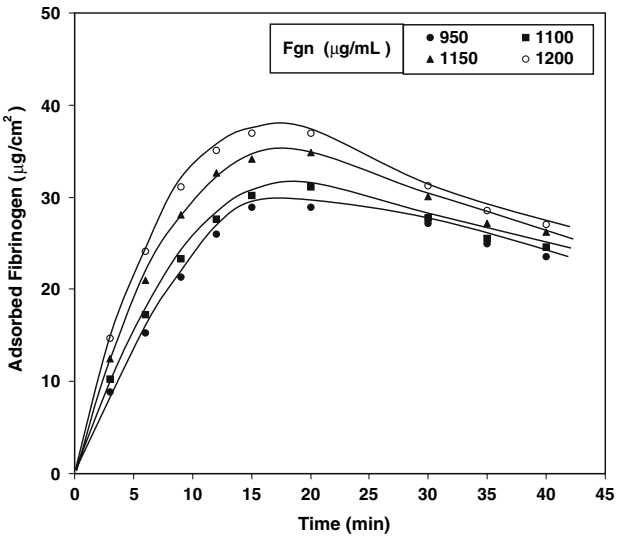

Fig. 8 Plots showing the progress of the adsorption from Fgn solution of higher concentrations on to the IPNs surfaces of definite composition [PEG] = 0.5 g, [HEMA] = 32.9 mM, [AN] = 48.6 mM, [EGDMA] = 1.06 mM, [Water] = 50% (v/v), [KPS] = 0.037 mM, [MBS] = 0.40 mM, pH = 7.4, Temp. = 37 ± 0.2 °C, Ionic strength = 0.001 M KNO_3

The diffusion-controlled nature of the adsorption process, as discussed previously, reveals that each collision between fibrinogen molecule and the sponge surface results in an adsorption event. The initial increase in adsorption with increasing bulk concentration of protein solution may obviously be due to the fact that greater number of fibrinogen molecules interact with the surface and adsorb reversibly with end-on orientation. It is important to note that due to end-on orientation of adsorbed fibrinogen molecules footprint size become small and consequently less contact is established between the sponge surface and the adsorbed segments of fibrinogen molecule, which eventually results in a reversible adsorption. It is well known that fibrinogen (mol. wt. 340,000–400,000 Da) is an exceptionally elongated molecule with an axial ratio (major axis : minor axis) of about 18:1. It contains about 10% charged residues and is negatively charged at pH 7.4 (IP about 5.1).

Now, at higher concentration (>850 μg/mL) of the protein solution the adsorbed fibrinogen molecules are forced to undergo conformational transition from end-on to side-on adsorption so that the footprint size of the adsorbed protein molecules increases. The increased contact with the sponge surface results in a firm binding to the surface, thus, changing the adsorption from reversible to irreversible one. It is interesting to realize here that due to side-on orientation of adsorbed fibrinogen molecules, the sponge surfaces are shielded from the other approaching molecules and, therefore, the adsorbed amount of fibrinogen decreases. The whole scheme of adsorption may be modeled as shown in Fig. 9.

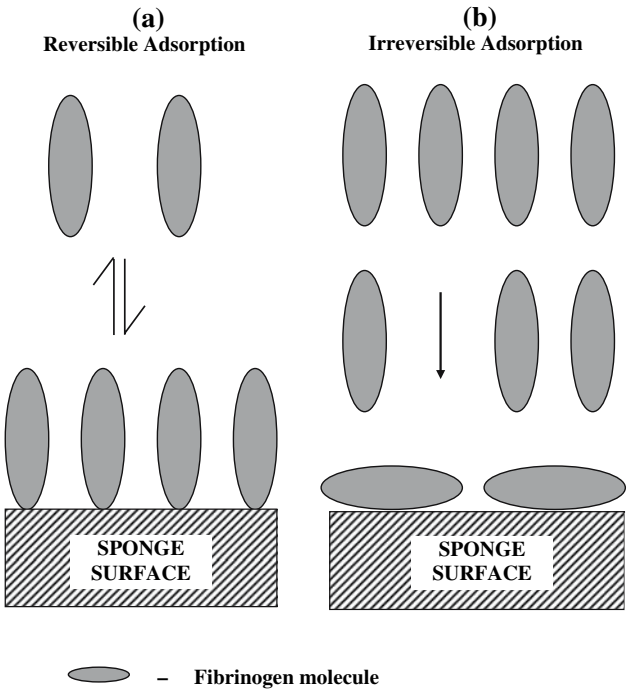

Fig. 9 A hypothetical kinetic model depicting the mechanism of Fgn adsorption at (**a**) lower and, (**b**) higher bulk concentration of protein solution

Table 5 Data showing the adsorption of Fgn onto the semi-IPN in the presence of various simulated biological fluids (Composition of semi-IPN is same as given in Table 3)

Physiological fluid	Adsorbed amount (μg/cm^2)
Phosphate buffer saline (PBS, pH 7.4)	26.2
KI (15% w/v)	24.2
Urea (5% w/v)	15.6
D-glucose (5% w/v)	16.7
Saline water (0.9% NaCl, w/v)	15.2
Synthetic Urine[a]	14.4

[a] NaCl (0.8% w/v, $MgSO_4$ (0.10% w/v), Urea (21 % w/v) and $CaCl_2$ (0.06% w/v)

Effect of solution and biological fluids

The influence of solute and media on the adsorption of fibrinogen was examined by performing adsorption experiments in presence of solutes such as potassium iodide (15% w/v), urea, and D-glucose (5% w/v), and in physiological fluids such as saline water (0.9% NaCl) and artificial urine. The adsorption results are presented in Table 5, which clearly reveal that in all the cases, a fall in adsorbed amount is noticed. The observed results can be explained by the fact that the salt ions present in the adsorption media also compete with the adsorbing fibrinogen molecules and thus partially exhaust available active sites on the sponge surfaces. This obviously results in a fall in the adsorption of fibrinogen.

Effect of IPN composition on Fgn adsorption

It has been largely noticed that the composition and organization of the adsorbed protein layer can be varied by numerous factors relating to the substrate, such as hydrophobicity, sorbed water content, microphase separation, and surface chemical functionality. As far as the chemistry of surfaces is concerned, the effect of hydrophilic and hydrophobic balance of constituent chains in polymer surfaces has been found to play a key role in influencing protein adsorption and subsequent platelet adhesion to polymer surfaces [61]. In general, a hydrophobic surface offers greater affinity for protein adsorption then that by a hydrophilic surface and this has been confirmed by a number of investigators also [62]. For example, Higuchi et al. [63] modified hydrophobic surfaces of polysulfone with poly(*N*-vinyl-2-pyrrolidone) and noticed a significant fall in platelet adhesion. Similarly, surface grafting with tethered brushes of hydrophilic polymers, such as

poly(ethylene glycol) have been shown to achieve minimal interaction with proteins and platelets [64]. Both flexibility and hydrophilicity are thought to play an essential role in this reduced interaction of brushed surfaces with blood components due to a steric repulsion mechanism. On the other hand, microarchitecture of material surface is also found to affect the protein–material interaction substantially.

When the water content in the polymerization system increases from 50% to 64% (v/v), the amount of adsorbed Fgn increases as summarized in Table 6. The reason for the observed increase may be attributed to the fact that in the presence of water phase separation begins due to thermodynamically unfavourable interaction between water and polymer which gives rise to network consisting of spheroidal particles surrounded by interconnected channels occupied by water. On increasing the proportion of water in the polymerization mixture, the onset of phase separation becomes fast and, therefore, the pore sizes of the IPN decreases whereas the equilibrium water content increases. Thus, due to increased water content and reduced pore size the adsorption of Fgn decreases.

When the concentration of PEG increases in the IPN in the range 0.5–2.0 g, the amount of adsorbed Fgn is found to decrease constantly in the studied range as summarized in Table 6. The lower affinity of PEG towards protein adsorption is well recognized and has been largely reported in the literature. The observed lower adsorption with increasing PEG may be attributed to the 'protein resistant' property of the polymer which may be explained by the fact that due to a hydrophilic nature of PEG it forms effective hydrogen bonds with water and thus formed structured water layer opposes protein adsorption onto the polymer surfaces. The 'protein resistant' property of the PEG can be well described in terms of 'steric stabilization effect' and 'chain mobility' as discussed elsewhere [65].

Table 6 Data showing the effect of varying compositions of the PEG-P(HEMA-co-AN) semi IPN and water content on the adsorption of Fgn

Water content (%) v/v	PEG (g)	HEMA (mM)	AN (mM)	EGDMA (mM)	Adsorbed protein (μg/cm^2)
50	0.5	32.9	48.6	1.06	26.2
55	0.5	32.9	48.6	1.06	22.0
60	0.5	32.9	48.6	1.06	18.5
64	0.5	32.9	48.6	1.06	12.5
50	0.5	32.9	48.6	1.06	26.2
50	1.0	32.9	48.6	1.06	19.9
50	1.5	32.9	48.6	1.06	13.5
50	2.0	32.9	48.6	1.06	8.43
50	0.5	16.4	48.6	1.06	46.2
50	0.5	24.6	48.6	1.06	31.5
50	0.5	32.9	48.6	1.06	26.2
50	0.5	41.1	48.6	1.06	22.7
50	0.5	32.9	16.2	1.06	52.6
50	0.5	32.9	32.4	1.06	33.8
50	0.5	32.9	48.6	1.06	26.2
50	0.5	32.9	64.8	1.06	17.7
50	0.5	32.9	48.6	0.53	28.9
50	0.5	32.9	48.6	1.06	26.2
50	0.5	32.9	48.6	1.59	34.6
50	0.5	32.9	48.6	2.12	43.5

In the present study the effect of HEMA content in the IPNs on the adsorbed amount of Fgn has been investigated by varying the concentration of HEMA in the range 24.6–49.3 mM. The results are shown in Table 6 which clearly imply that the amounts of adsorbed Fgn significantly decreases with increasing HEMA in the feed mixture of the sponges. The observed results could be explained by the fact that with increasing PHEMA content in the IPN the network chains acquire a compact arrangement, thus resulting in a shrinkage of the pore sizes of polymer network. A reduction in pore size of the sponge obviously restricts the diffusion of large Fgn molecules into the IPN pores and thus a decrease in the adsorbed Fgn in noticed.

The amount of polyacrylonitrile content in the IPN has also been found to affect Fgn adsorption as shown in Table 6. The results clearly reveal that as the acrylonitrile concentration increases, the adsorbed Fgn decreases which may be attributed to the reason that with increasing AN, the IPN shows a greater water uptake and, therefore, the adsorption of protein decreases.

The crosslinking agent employed in the present study was EGDMA which is a known hydrophobic crosslinker. The influence of EGDMA on the protein adsorption has been investigated by increasing its concentration in the IPNs in the ranges 0.53–2.12 mM. The results are shown in Table 6, which reveal that the adsorbed Fgn increases with increasing EGDMA concentration in the IPN. The increase in the Fgn adsorption can be attributed to the fact that hydrophobic domains of Fgn interact with the hydrophobic segments of the crosslinker EGDMA and thus cause adsorption of Fgn on the sponge surfaces as a result of entropic hydrophilic interactions and lyophilic liquid binding capabilities. Similar type of results have also been published by other workers [66]. It is worth mentioning here that the water content is not only important, but also the surface mobility and volume restriction which, consequently determine the state of water (degree of free water fraction over restricted water), a critical factor influencing blood interactions at polymer surfaces.

Blood clot formation and hemolysis

A great deal of experimental work has been confined to fabricate a biomaterial that lasts long without failure when put in contact with a stream of flowing blood under in vivo conditions. The fundamental approach behind the above task has been to minimize the extent of thrombus formation on blood-contacting devices thus to synthesize a non-thrombogenic polymer. The rationale for the development of these non-thrombogenic polymers is to prevent activation of the thrombogenic pathway by tailoring polymer surfaces to minimize blood interaction. An alternative route to achieve a non-thrombogenic polymeric implants has been to design a material with very low affinity for protein adsorption since, as mentioned earlier also, a thin layer of protein is formed at the blood-material interface within a few seconds after flowing blood contacts a foreign surface. Subsequent cellular events, such as adhesion and aggregation of platelets that initiate clot formation are most likely mediated by this protein layer instead of by the material surface itself. As different surfaces show different affinity for protein adsorption, the clot formation may also be a function of the chemical architecture of the materials and their surface as well.

The clot formation and percent hemolysis data are presented in Table 7 which clearly reveal that with variation in the composition of the IPNs, the weight of the blood clot as well as percent hemolysis also vary. It can be clearly seen in the table that whereas an increase in the PEG, AN and HEMA concentration in the reaction mixture has resulted in the IPNs with lower amount of clot formed and hemolysis, a higher weight of blood-clot and hemolysis were found with increased crosslinker (EGDMA) concentration. The obtained results suggest that antithrombogenic potential of a material is combinedly determined by hydrophilic, hydrophobic and protein adsorbing nature of the material.

Table 7 Data showing the amounts of blood-clot formed and % hemolysis with varying compositions of the IPNs surfaces

PEG (g)	HEMA (mM)	AN (mM)	EGDMA (mM)	Weight of blood-clot (mg)	% Hemolysis
0.5	32.9	48.6	1.06	6.8	12.2
1.0	32.9	48.6	1.06	5.0	10.6
1.5	32.9	48.6	1.06	3.6	8.8
2.0	32.9	48.6	1.06	2.4	8.0
0.5	16.4	48.6	1.06	9.8	16.3
0.5	24.6	48.6	1.06	8.4	14.4
0.5	32.9	48.6	1.06	6.8	12.2
0.5	41.1	48.6	1.06	4.2	10.2
0.5	32.9	16.2	1.06	8.4	15.3
0.5	32.9	32.4	1.06	7.2	14.0
0.5	32.9	48.6	1.06	6.8	12.2
0.5	32.9	64.8	1.06	3.8	9.8
0.5	32.9	48.6	0.53	5.2	11.2
0.5	32.9	48.6	1.06	6.8	12.2
0.5	32.9	48.6	1.59	8.2	14.2
0.5	32.9	48.6	2.12	10.4	18.4
Glass surface				42.4	31.4

Conclusions

Polymerization of HEMA and AN in the presence of a crosslinker (EGDMA) and a preformed polymer such as PEG produces a hydrophilic semi-interpenetrating polymer network (IPN) which display water uptake property. The degree of water sorption was found to decrease with increasing concentrations of PEG, HEMA and EGDMA while an increase in the swelling of the IPN was noticed with increasing concentration of AN. The semi-IPN was characterized by FTIR spectra and Environmental Scanning Electron Microscopy and various structural parameters such as average molecular weight between crosslinks, crosslink density and number of elastically effective chains were determined.

The adsorption of fibrinogen onto the IPNs surface is found to follow Langmuir isotherm equation. The amount of adsorbed fibrinogen increases with increasing concentration of HEMA and EGDMA while it decreases with increasing AN and PEG. The adsorption attains an optimum value at the isoelectric pH of the protein and gets shifted to the acidic pH range when ionic strength of the protein solution is increased. The adsorption of Fgn is also suppressed in simulated biological media.

The Fgn molecules adsorb onto the IPNs surfaces via a three step mechanism, i.e., diffusion, attachment to the surface, and reconformation. The IPNs synthesized display a fair degree of antithrombogenicity which is jointly determined by the hydrophilic, hydrophobic and protein adsorbing nature of the biomaterial. In particular, it is found that with increasing content of PEG, PHEMA and AN in the IPNs the antithrombogenic property of the polymer matrix also increases while on increasing the concentration of crosslinker (EGDMA) a fall in antithromobgenicity is noticed.

References

1. J. B. PARK and J. D. BRONZIONI, *Biomaterials: Principles And Applications* (Boca Raton: CRC Press LLC, 2003)
2. B. D. RATNER and S. J. BRYANT, *Annu. Rev. Biomed. Eng.* **6** (2004) 41
3. J. M. ANDERSON, *Annu. Rev. Mater. Res.* **31** (2001) 81

4. T. O. COLLIER and J. M. ANDERSON, *J. Biomed. Mater. Res.* **60** (2002) 487
5. T. A. HORBETT, *Surf. Sci. Ser.* **110** (2003) 393
6. J. J. GRAY, *Curr. Opin. Stru. Biology* **14** (2004) 10
7. A. R. JAHANGIR, W. G. MCCLUNG, R. M. CORNELIUS, C. B. MCCLOSKEY, J. L. BRASH and J. P. SANTERRE, *Biomed. Mater. Res.* **60** (2002) 135
8. W. B. TSAI, J. M. GRUNKEMEIER and T. A. HORBETT, *J. Biomed. Mater. Res.* **67A** (2003) 1255
9. S. BEGUIN and R. KUMAR, *Thromb. Haemost.* **78** (1997) 590
10. J. GRUNKEMEIER and T. HORBETT, *J. Mol. Recognit.* **9** (1996) 247
11. F. MARKWARDT, *Thromb. Haemost.* **66** (1991) 141
12. E. VOGLER, J. GRAPER, G. HARPER, H. SUGG, L. LANDER and W. BRITTAIN, *Biomed. Mater. Res.* **29** (1995) 1005
13. L. E. S. BRINK, S. J. G. ELBERS, T. ROBERTSEN and P. BOTH, *J. Membr. Sci.* **76** (1993) 281
14. C. G. P. H. SCHOREN, M. C. WIJERS, M. A. COHEN-STUART, VANDER PADT and R.K. VANT, *J. Membr. Sci.* **80** (1993) 265
15. M. AMIJI and K. PARK, *Biomaterials* **13** (1992) 682
16. J. H. LEE, P. A. MARTIK and T. S. TAN, *J. Colloid Interface Sci.* **131** (1989) 252
17. H. DU, P. CHOUDHARY and S. W. HUI, *Biochim. Biophys. Acta* **1326** (1997) 236
18. M. HANSON, K. K. UNGER, C. T. MANT and R. S. HOGDES, *J. Chromatogr.* **599** (1992) 65
19. M. GILGES, M. H. KLEEMISS and G. SCHOMBURG, *Anal. Chem.* **66** (1994) 2038
20. C. L. NG, H. K. LEE and S. F. Y. LI, *J. Chromatogr.* **A659** (1994) 427
21. J. S. TAN and P. A. MARTIC, *J. Colloid Interface Sci.* **136** (1990) 415
22. M. MAMESTERN, P. LINSE and T. COSGROVE, *Macromolecules* **25** (1992) 2474
23. F. F. STENGAARD, *Desalination* **70** (1988) 207
24. S. AKHTAR, C. HOWES, L. DUDLEY, I. REED and P. STATFORD, *J. Membr. Sci.* **107** (1995) 209
25. D. S. JONES, M. C. BONNER, S. P. GORMAN, M. AKAY and P. F. KEANE, *J. Mater. Sci. Mater. Med.* **8** (1997) 713
26. G. A. ABRAHAM, A. A. A. de QUEIROZ and J. S. ROMAN, *Biomaterials* **22** (2001) 1971
27. K. M. HANSSON, S. TOSATTI, J. ISAKSSON, J. WETTERO, M. TEXTOR, T. L. LINDAHL and P. TENGVALL, *Biomaterials* **26** (2005) 861
28. J. ANDRADE, U. HLADY, A.-P. WEI, C.-H. HO, A. LECA, S. JEON, Y. LIN and E. STRAUP, *J. Clin. Mater.* **11** (1992) 67
29. L. FLYNN, P. D. DALTON and M. S. SHOICHET, *Biomaterials* **24** (2003) 4265
30. P. D. DALTON, L. FLYNN and M. S. SHOICHET, *Biomaterials* **23** (2002) 3843
31. A. M. DEEPAK and K. ASHWANI, *J. Appl. Polym. Sci.* **77** (2000) 1782
32. A. K. BAJPAI and M. SHRIVASTAVA, *J. Macromol. Sci. Pure Appl. Chem.* **A38** (2001) 1123
33. A. K. BAJPAI and D. D. MISHRA, *J. Mater. Sci. Mater. Med.* **15** (2004) 583
34. D. G. CASTNER and B. D. RATNER, *Surf. Sci.* **1–3** (2002) 28
35. A. S. HOFFMAN, *Adv. Drug Del. Rev.* **43** (2002) 3
36. Y. IMAI and Y. NOSE, *J. Biomed. Mater. Res.* **6** (1972) 165
37. D. K. SINGH and A. K. RAY, *J. Appl. Polym. Sci.* **53** (1994) 1115
38. P. J. FLORY and J. REHNER, *J. Chem. Phys.* **11** (1943) 521
39. D. A. PULEO and A. NANCI, *Biomaterials* **20** (1999) 2311
40. D. M. BRUNNETTE, *Int. J. Oral Maxillofac Implants* **3** (1988) 231
41. P. KORBELAR, J. VACIK and I. DYLEVSKY, *J. Biomed. Mater. Res.* **22** (1988) 751
42. B. RAMARAJ and G. RADHKRISHNAN, *Polymer* **35** (1994) 2167
43. J. ISRAELACHVILI, *Intermolecular and Surface Forces*, 2nd edn. (Academic Press, London, 1992)
44. M. MORRA, *J. Biomater. Sci. Polym. Ed.* **11** (2000) 547
45. M. R. OBERHOLZER, A. M. LENHOFF, *Langmuir* **15** (1999) 3905
46. Z. ADAMCZYK, P. WERONSKI and E. MUSIAL, *Colloids Surf.: Physicochem. Eng. Aspects* **208** (2002) 29
47. M. A. BRUSATORI and P. R. van TASSEL, *J. Colloid. Interface Sci.* **219** (1999) 333
48. J. STAHLBERG and B. JONSSON, *Anal. Chem.* **68** (1996) 1536
49. F. FANG and I. SZLEIFER, *Biophys. J.* **80** (2001) 2568
50. C. M. ROTH and A. M. LENHOFF, *Surf. Sci. Ser.* **75** (1998) 89
51. N. KAYIRHAN, A. DENIZLI and N. HASIRCI, *J. Appl. Polym. Sci.* **81** (2001) 1322
52. A. K. BAJPAI, *Polym. Int.* **53** (2004) 261
53. J. C. DIJIT, M. A. COHEN STUART, J. F. HOFFMAN and G. J. FLEER, *Colloids Surf.* **51** (1990) 141
54. D. F. SIQUERIA, U. BREINER, R. STADLER and M. STAMM, *Langmuir* **12** (1996) 972
55. C. LIGOURO and L. LEIBLER, *J. Phys. (Paris)* **51** (1990) 1313
56. M. TANAKA, A. MOCHIZAKI, T. SHIROYA, T. MOTOMURA, K. SHIMURA, M. ONISHI and Y. OKAHATA, *Colloids Surf. (A): Physicochem. Eng. Aspects* **203** (2002) 195
57. C. F. WERTZ and M. M. SANTORE, *Langmuir* **17** (2001) 3006
58. C. F. WERTZ and M. M. SANTORE, *Langmuir* **15** (1999) 8884
59. F. MACRITCHIE, *J. Colloid Interface Sci.* **38** (1972) 484
60. C. F. WERTZ and M. M. SANTORE, *Langmuir* **18** (2002) 706
61. Y.-X. WANG, J. L. ROBERTSON, W. B. SPILLMAN Jr. and R. O. CLAUS, *Pharmaceut. Res.* **21**(8) (2004) 1362
62. D. L. ELBERT and J. A. HUBELL, *Annu. Rev. Mater. Sci.* **26** (1996) 365
63. A. HIGUCHI, K. SHIRANO, M. HARSHIMA, M. YOON, M. HARA, M. HATTORI and K. IMAMURA, *Biomaterials* **23** (2002) 2659
64. N. HUANG, J. VOROS, S. DEPAUL, M. TEXTOR and N. SPENCER, *Langmuir* **18** (2002) 220
65. F. ZHANG, E. T. KANG, K. G. NEOH, P. WANG and K. L. TARR, *Biomaterials* **23** (2002) 787
66. D. GRAINGER, T. OKANO and S. W. KIM, In *Advances in Biomedical Polymers*, edited by C. G. Gebelein (Plenum Press, New York, 1987)